Bulletin of Electrical Engineering and Informatics
Vol. 10, No. 1, February 2021, pp. 241∼248
ISSN: 2302-9285, DOI: 10.11591/eei.v10i1.2102

Employing non-orthogonal multiple access scheme in UAV-based wireless networks

Chi-Bao Le[1], **Dinh-Thuan Do** [2]
[1]Faculty of Electronics Technology, Industrial University of Ho Chi Minh City (IUH), Vietnam
[2]Wireless Communications Research Group, Faculty of Electrical and Electronics Engineering, Ton Duc Thang University, Vietnam

Article Info

Article history:

Received Oct 27, 2019
Revised Apr 3, 2020
Accepted Jun 25, 2020

Keywords:

NOMA
Outage Probability
UAV

ABSTRACT

This paper studies the two-hop transmission relying unmanned aerial vehicle (UAV) relays which is suitable to implement in the internet of things (IoT) systems. To enhance system performance in order to overcome the large scale fading between the base station (BS) and destination as well as achieve the higher spectrum efficiency, where non-orthogonal multiple access (NOMA) strategies were typically applied for UAV relays to implement massive connections transmission. In particular, outage probability is evaluated via signal to noise ratio (SNR) criterion so that the terminal node can obtain reasonable performance. The derivations and analysis results showed that the considered fixed power allocation scheme provides performance gap among two signals at destination.The numerical simulation confirmed the exactness of derived expressions in the UAV assisted system.

Corresponding Author:

Dinh-Thuan Do,
Wireless Communications Research Group,
Faculty of Electrical and Electronics Engineering,
Ton Duc Thang University, Ho Chi Minh City, Vietnam.
Email: dodinhthuan@tdtu.edu.vn

1. INTRODUCTION

Wireless communication technology has pace to adapt demand with rapid development of new techniques. The decreasing cost of unmanned aerial vehicle (UAV) network together with the dramatical innovation of UAV-based manufacturing technology provides connections as some difficulties happen. Therefore, some applications such as weather monitoring systems, forest fire prevention technology, man-v-machine are provided by many new UAV applications appeared in the civilian market. In order to implement the UAV relay based IoT networks, wide range of applications of UAV-based network attracts more attentions from community of researchers [1]. Recently, to achieve throughput transmission above 10Gbps, ultra density device connection and millisecond transmission delay, implement of 5G/B5G networks needs UAV assisted communications as reported in [2, 3]. The network coverage expands to 3D interconnection as crucial demand for development of the future communications and it releases the large scale fading regarding very high speed transmission. Moreover, higher cost and difficulty in the construction of cellular stations happen and such situation leads to solutions of the IoT network by employing the UAV relays assisted Communication. UAV-based network benefits to infrastructure development by providing itss convenient implement and lower cost, high-altitude assisted transmission [4, 5]. The main advantages of the UAV relay assisted communications are reducing the obstruction from buildings, mountains and archieving the higher line of sight (LoS) transmission effect [6, 7].

Due to ability of massive connections and higher spectrum efficiency, NOMA has attracted great research interest from both academia and industry [8–24]. Since users aware on imperfect channel state information (CSI), the author studied the impact of imperfect CSI on the performance of NOMA in [15]. In [16], the throughput aspects of the cognitive radio as applying NOMA techniques were discussed and compared.

2. SYSTEM MODEL

Figure 1 shows system model containing the two-hop transmission using UAV relay communication model. Two UAV relays operate in half duplex and DF mode to signal forwarding, while separated signal is detected at destination. The terminal IoT node receives signal from two links as shown in Figure 1. Typically, the obstacles or blockage of urban buildings and mountains limit quality of the communication between the base station BS and terminal node D, then the UAV relays are implemented to realize assisted communication. The destination user needs two phases to perform its the transmission process. In the first phase, the BS transmits mixture signal to the two UAV relay nodes R_1, R_2. The channels h_i between the BS and the UAV relays follow Nakagami-m distribution.

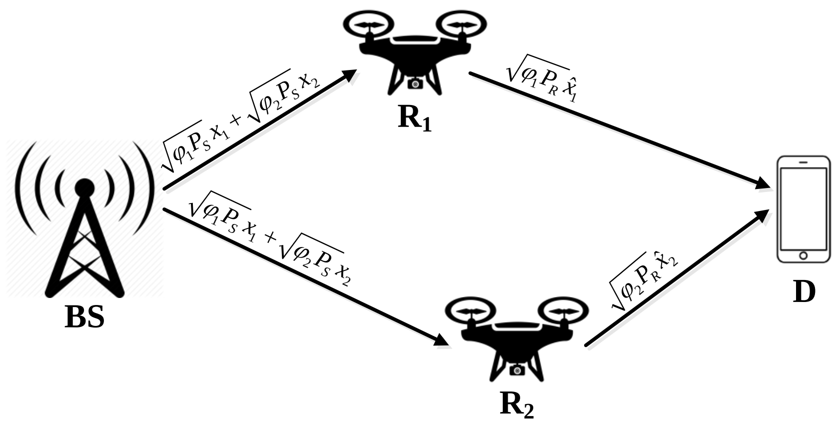

Figure 1. System model of UAV-assisted NOMA.

The received signal at UAV relays are given as

$$y_i = h_i \left(\sqrt{\varphi_1 P_S}x_1 + \sqrt{\varphi_2 P_S}x_2\right) \quad , i \in \{1, 2\}. \tag{1}$$

The signal to noise ratio (SNR) is used to dectect x_2 as

$$\Gamma_{R_1,x_2} = \frac{\varphi_2 \rho |h_1|}{\varphi_1 \rho |h_1| + 1}, \tag{2}$$

where $\rho = \frac{P_S}{N_0} = \frac{P_R}{N_0}$ is the transmit signal to noise radio (SNR).
After SIC happens, SNR is given to detect signal x_1 as

$$\Gamma_{R_1,x_1} = \varphi_1 \rho |h_1|. \tag{3}$$

Similarly, SNR at R_2 to detect x_2 is given as

$$\Gamma_{R_2,x_2} = \frac{\varphi_2 \rho |h_2|}{\varphi_1 \rho |h_2| + 1}. \tag{4}$$

Next, we will introduce the channel model of $R_i \rightarrow D$ link. In general, the UAV coverage is a circular cell and the UAV is located at the vertical center. Thus, the channel vector of $R_i \rightarrow D$ link can be expressed as

$$g_i = L_i \bar{g}_i \quad , i \in \{1, 2\}, \tag{5}$$

where the free space loss of the path L_i is given by

$$L_i = \frac{\lambda_u}{4\pi\sqrt{d_{R_i}^2 + d_h^2}}, \tag{6}$$

where d_h and d_{R_i} denote the height of UAV relay and the distance from the center of two UAV relay's to D, respectively, λ_u represents the wavelength.

Then, in the second phase of communication, each UAV relay forwards detected symbols to the destination (uplink-NOMA) and the received signal at user is given as

$$y_D = \sqrt{P_R}\left(\sqrt{\varphi_1}\hat{x}_1 L_1 \bar{g}_1 + \sqrt{\varphi_2}\hat{x}_2 L_2 \bar{g}_2\right). \tag{7}$$

where P_R is the normalized transmission powers at two relay's

It can be computed SNR at user D to detect signal $x2$ is

$$\Gamma_{D,x_2} = \frac{\rho\varphi_2 L_2^{-2}|g_2|^2}{\rho\varphi_1 L_1^{-2}|g_1|^2 + 1}. \tag{8}$$

Then, SNR at user D is calculated to detect signal x_1 is

$$\Gamma_{D,x_1} = \rho\varphi_1 L_1^{-2}|g_1|^2. \tag{9}$$

3. PERFORMANCE ANALYSIS

3.1. Outage probability of x_1

At destination, user D needs detect its signals. However, these signals are evaluated via outage probability. Such outage is defined as probability to SNR less than the pre-defined threshold SNR. We first consider outage performance of x_1 as below:

$$\begin{aligned}
\mathcal{P}_{x_1} =& \Pr\left(\Gamma_{R_1,x_2} < \varepsilon_2 \cup \Gamma_{R_1,x_1} < \varepsilon_1 \cup \Gamma_{D,x_2} < \varepsilon_2 \cup \Gamma_{D,x_1} < \varepsilon_1\right) \\
=& 1 - \Pr\left(\Gamma_{R_1,x_2} \geq \varepsilon_2 \cup \Gamma_{R_1,x_1} \geq \varepsilon_1 \cup \Gamma_{D,x_2} \geq \varepsilon_2 \cup \Gamma_{D,x_1} \geq \varepsilon_1\right) \\
=& 1 - \underbrace{\Pr\left(|h_1| \geq \chi\right)}_{\mathcal{A}_1} \underbrace{\Pr\left(|g_2|^2 \geq \delta|g_1|^2 + \varpi_2, |g_1|^2 \geq \varpi_1\right)}_{\mathcal{A}_2},
\end{aligned} \tag{10}$$

where $\varepsilon_1 = 2^{2R_1} - 1$ with R_1 being the target rate at D to detect x_1, $\varepsilon_2 = 2^{2R_2} - 1$ with R_2 being the target rate at D to detect x_2, $\chi = \max\left(\frac{\varepsilon_2}{\rho(\varphi_2 - \varepsilon_2\varphi_1)}, \frac{\varepsilon_1}{\varphi_1\rho}\right)$, $\delta = \frac{\varepsilon_2\varphi_1 L_1^{-2}}{\varphi_2 L_2^{-2}}$, $\varpi_1 = \frac{\varepsilon_1}{\rho\varphi_1 L_1^{-2}}$ and $\varpi_2 = \frac{\varepsilon_2}{\rho\varphi_2 L_2^{-2}}$

Let $Z_i = \left\{|h_i|^2, |g_i|^2\right\}$, $i \in \{1, 2\}$ and we set, The CDFs and PDFs of Z

$$F_{Z_i}(x) = 1 - e^{-\mu_{z_i}x}\sum_{s=0}^{m_{z_i}-1}\frac{\mu_{z_i}^s x^s}{s!}, \tag{11}$$

and

$$f_{Z_i}(x) = \frac{\mu_{Z_i}^{m_{Z_i}} x^{m_{Z_i}-1} e^{-\mu_{Z_i}x}}{\Gamma(m_{Z_i})}, \tag{12}$$

where $\mu_{z_i} = \frac{m_{z_i}}{\lambda_{z_i}}$

$$\begin{aligned}\mathcal{A}_1 =& \Pr\left(|h_1| \geq \chi\right)\\ =& 1 - F_{|h_1|}\left(\chi\right)\\ =& e^{-\mu_{h_1}\chi}\sum_{a=0}^{m_{h_1}-1}\frac{\mu_{h_1}^a\chi^a}{a!}.\end{aligned} \tag{13}$$

Then, $\mathcal{A}_2$ is given by

$$\begin{aligned}\mathcal{A}_2 =& \Pr\left(|g_2|^2 \geq \delta|g_1|^2 + \varpi_2, |g_1|^2 \geq \varpi_1\right)\\ =& \int\limits_{\varpi_1}^{\infty} f_{|g_1|^2}\left(x\right)\left[1 - F_{|g_2|^2}\left(\delta x + \varpi_2\right)\right]dx\\ =& \sum_{d=0}^{m_{g_2}-1}\frac{\mu_{g_2}^d\mu_{g_1}^{m_{g_1}}e^{-\mu_{g_2}\varpi_2}}{d!\Gamma\left(m_{g_1}\right)}\int\limits_{\varpi_1}^{\infty}x^{m_{g_1}-1}e^{-x\left(\mu_{g_1}+\mu_{g_2}\delta\right)}\left(\delta x+\varpi_2\right)^d dx\\ =& \sum_{d=0}^{m_{g_2}-1}\sum_{t=0}^{d}\left(\begin{array}{c}d\\t\end{array}\right)\frac{\mu_{g_2}^d\mu_{g_1}^{m_{g_1}}\varpi_2^{d-t}\delta^t e^{-\mu_{g_2}\varpi_2}}{d!\Gamma\left(m_{g_1}\right)}\int\limits_{\varpi_1}^{\infty}x^{m_{g_1}+t-1}e^{-x\left(\mu_{g_1}+\mu_{g_2}\delta\right)}dx.\end{aligned} \tag{14}$$

Applying [[23], (3.351.2)], $\mathcal{A}_2$ is given by

$$\mathcal{A}_2 = \sum_{d=0}^{m_{g_2}-1}\sum_{t=0}^{d}\sum_{k=0}^{m_{g_1}+t-1}\left(\begin{array}{c}d\\t\end{array}\right)\frac{\mu_{g_2}^d\mu_{g_1}^{m_{g_1}}\varpi_2^{d-t}\delta^t\Gamma\left(m_{g_1}+t\right)\varpi_1^k e^{-\mu_{g_2}\varpi_2-\varpi_1\left(\mu_{g_1}+\mu_{g_2}\delta\right)}}{d!k!\Gamma\left(m_{g_1}\right)\left(\mu_{g_1}+\mu_{g_2}\delta\right)^{m_{g_1}+t-k}} \tag{15}$$

where $\Gamma\left(x\right) = \left(x-1\right)!$ is the gamma function. Next, substituting (15) and (13) into (10), $\mathcal{P}_{x_1}$ is expressed by

$$\begin{aligned}\mathcal{P}_{x_1} =& 1 - e^{-\mu_{h_1}\chi}\sum_{a=0}^{m_{h_1}-1}\sum_{d=0}^{m_{g_2}-1}\sum_{t=0}^{d}\sum_{k=0}^{m_{g_1}+t-1}\left(\begin{array}{c}d\\t\end{array}\right)\frac{\mu_{g_2}^d\mu_{g_1}^{m_{g_1}}\mu_{h_1}^a\chi^a\varpi_2^{d-t}\delta^t\Gamma\left(m_{g_1}+t\right)\varpi_1^k}{a!d!k!\Gamma\left(m_{g_1}\right)}\\ &\times\frac{e^{-\mu_{g_2}\varpi_2-\varpi_1\left(\mu_{g_1}+\mu_{g_2}\delta\right)}}{\left(\mu_{g_1}+\mu_{g_2}\delta\right)^{m_{g_1}+t-k}}.\end{aligned} \tag{16}$$

When $\rho \to \infty$, by using $e^{-x} \approx 1 - x$ so the asymptotic of $\mathcal{P}_{x_1}^{\infty}$ is formulated by

$$\begin{aligned}\mathcal{P}_{x_1}^{\infty} =& 1 - \left(1 - \mu_{h_1}\chi\right)\sum_{a=0}^{m_{h_1}-1}\sum_{d=0}^{m_{g_2}-1}\sum_{t=0}^{d}\sum_{k=0}^{m_{g_1}+t-1}\left(\begin{array}{c}d\\t\end{array}\right)\frac{\mu_{g_2}^d\mu_{g_1}^{m_{g_1}}\mu_{h_1}^a\chi^a\varpi_2^{d-t}\delta^t\Gamma\left(m_{g_1}+t\right)\varpi_1^k}{a!d!k!\Gamma\left(m_{g_1}\right)}\\ &\times\frac{\left[1-\mu_{g_2}\varpi_2-\varpi_1\left(\mu_{g_1}+\mu_{g_2}\delta\right)\right]}{\left(\mu_{g_1}+\mu_{g_2}\delta\right)^{m_{g_1}+t-k}}.\end{aligned} \tag{17}$$

According to (8), we have $\lim\limits_{\rho\to\infty}\Gamma_{D,x_2} = \frac{\varphi_2 L_2^{-2}|g_2|^2}{\varphi_1 L_1^{-2}|g_1|^2}$ the approximate of $\mathcal{P}_{x_1}^{app.}$ and $\mathcal{P}_{x_2}^{app.}$ are given by

$$\mathcal{P}_{x_1}^{app.} = \mathcal{P}_{x_2}^{app.} = \sum_{d=0}^{m_{g_2}-1}\frac{\mu_{g_2}^d\mu_{g_1}^{m_{g_1}}\delta^d\Gamma\left(m_{g_1}+d\right)}{d!\Gamma\left(m_{g_1}\right)\left(\mu_{g_1}+\mu_{g_2}\delta\right)^{m_{g_1}+d}}. \tag{18}$$

3.2. Outage probability of x_2

Similarly, outage performance of x_2 can be formulated by

$$\begin{aligned}\mathcal{P}_{x_2} &= \Pr\left(\Gamma_{R_2,x_2} < \varepsilon_2 \cup \Gamma_{D,x_2} < \varepsilon_2\right)\\ &= 1 - \Pr\left(\Gamma_{R_2,x_2} \ge \varepsilon_2, \Gamma_{D,x_2} \ge \varepsilon_2\right)\\ &= 1 - \underbrace{\Pr\left(|h_2| \ge \nu\right)}_{\mathcal{B}_1}\underbrace{\Pr\left(|g_2|^2 \ge \delta|g_1|^2 + \varpi_2\right)}_{\mathcal{B}_2},\end{aligned} \tag{19}$$

where $\nu = \frac{\varepsilon_2}{\rho(\varphi_2 - \varepsilon_2\varphi_1)}$

We need compute each outage component as

$$\begin{aligned}\mathcal{B}_1 &= \Pr\left(|h_2| \ge \nu\right)\\ &= 1 - F_{|h_2|}\left(\nu\right)\\ &= e^{-\mu_{h_2}\nu}\sum_{b=0}^{m_{h_2}-1}\frac{\mu_{h_2}^b \nu^b}{b!}.\end{aligned} \tag{20}$$

Then, we continue to compute the second term as

$$\begin{aligned}\mathcal{B}_2 &= \Pr\left(|g_2|^2 \ge \delta|g_1|^2 + \varpi_2\right)\\ &= \int_0^\infty f_{|g_1|^2}\left(x\right)\left[1 - F_{|g_2|^2}\left(\delta x + \varpi_2\right)\right]dx\\ &= \sum_{d=0}^{m_{g_2}-1}\sum_{t=0}^{d}\binom{d}{t}\frac{\mu_{g_2}^d \mu_{g_1}^{m_{g_1}}\delta^t \varpi_2^{d-t} e^{-\mu_{g_2}\varpi_2}}{d!\Gamma\left(m_{g_1}\right)}\int_0^\infty x^{m_{g_1}+t-1}e^{-x\left(\mu_{g_1}+\mu_{g_2}\delta\right)}dx.\end{aligned} \tag{21}$$

Based on [[17], (3.351.3)], $\mathcal{B}_2$ is given by

$$\mathcal{B}_2 = \sum_{d=0}^{m_{g_2}-1}\sum_{t=0}^{d}\binom{d}{t}\frac{\mu_{g_2}^d \mu_{g_1}^{m_{g_1}}\delta^t \varpi_2^{d-t}\Gamma\left(m_{g_1}+t\right)e^{-\mu_{g_2}\varpi_2}}{d!\Gamma\left(m_{g_1}\right)\left(\mu_{g_1}+\mu_{g_2}\delta\right)^{m_{g_1}+t}}. \tag{22}$$

Substituting (22) and (20) into (19), $\mathcal{P}_{x_2}$ is given by

$$\mathcal{P}_{x_2} = 1 - e^{-\mu_{h_2}\nu}\sum_{b=0}^{m_{h_2}-1}\sum_{d=0}^{m_{g_2}-1}\sum_{t=0}^{d}\binom{d}{t}\frac{\mu_{h_2}^b \nu^b \mu_{g_2}^d \mu_{g_1}^{m_{g_1}}\delta^t \varpi_2^{d-t}\Gamma\left(m_{g_1}+t\right)e^{-\mu_{g_2}\varpi_2}}{b!d!\Gamma\left(m_{g_1}\right)\left(\mu_{g_1}+\mu_{g_2}\delta\right)^{m_{g_1}+t}}. \tag{23}$$

Corresponding to formula (17) the asymptotic of $\mathcal{P}_{x_2}^\infty$ is given by

$$\mathcal{P}_{x_2}^\infty = 1 - \left(1 - \mu_{h_2}\nu\right)\sum_{b=0}^{m_{h_2}-1}\sum_{d=0}^{m_{g_2}-1}\sum_{t=0}^{d}\binom{d}{t}\frac{\mu_{h_2}^b \nu^b \mu_{g_2}^d \mu_{g_1}^{m_{g_1}}\delta^t \varpi_2^{d-t}\Gamma\left(m_{g_1}+t\right)\left(1-\mu_{g_2}\varpi_2\right)}{b!d!\Gamma\left(m_{g_1}\right)\left(\mu_{g_1}+\mu_{g_2}\delta\right)^{m_{g_1}+t}}. \tag{24}$$

4. NUMERICAL RESULTS

We set fading parameter $m = m_{h_1} = m_{h_2} = m_{g_1} = m_{g_2} = 2$ and channel gains as $\lambda = \lambda_{h_1} = \lambda_{h_2} = \lambda_{g_1} = \lambda_{g_2} = 1$. The power allocation coefficients of NOMA's users are $\varphi_1 = 0.1$ and $\varphi_1 = 0.9$. The target rates are R_1 and R_2 and they are set to be $R_1 = R_2 = 0.5$. The times of Monte Carlo simulation 10^7. The height of UAV $d_h = 300\,\mathrm{m}$. The distance between $R_1 \to D$ and $R_2 \to D$ are $d_{R_1D} = 200\,\mathrm{m}$ and $d_{R_1D} = 100\,\mathrm{m}$, respectively.

Figure 2 shows outage performance versus transmit SNR. We consider four cases of m. As can be seen from such outage performance, asymptotic curves are very matched with exact curves. Signal x_2 exhibits better outage probability compared with x_1 since different power allocated to each signal. The simulation results are also very tight with the analytical results. $m = 4$ is considered as the best case among these curves.

Figure 3 confirms that NOMA benefits to outage performance of signal x_2 as it is better than OMA method. Figure 4 indicates the optimal outage for signal x_1 and it happens at $\varphi_1 = 0.25$. Higher threshold SNR results in worse outage performance of two signals as observation from Figure 5.

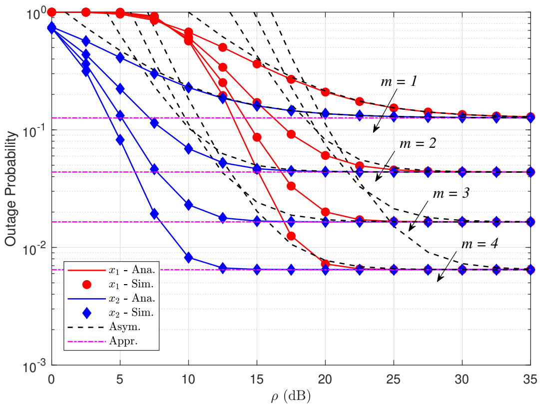

Figure 2. Outage performance of x_1 and x_2 versus transmit SNR

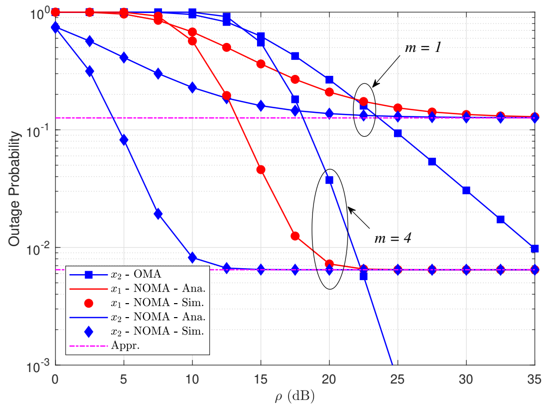

Figure 3. Comparison between OMA and NOMA

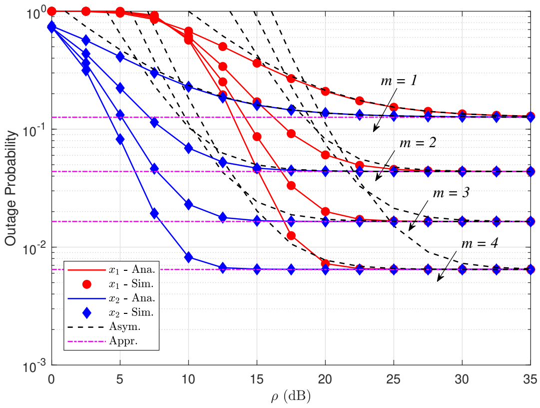

Figure 4. Outage performance versus φ_1, with $\rho = 10dB$

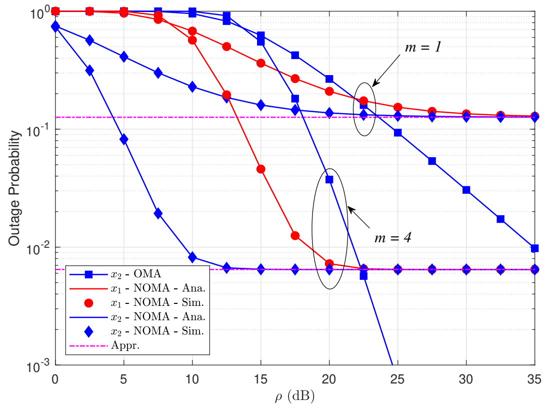

Figure 5. Outage performance versus threshold rates, with $\varphi_1 = 0.05$, $\varphi_2 = 1.95$ and $\rho = 20dB$

5. CONCLUSION

The paper proposed IoT system relying UAV relay to enhance performance of destination. This technique effectively overcomes the large scale fading between the BS and far user. Moreover, the proposed NOMA strategy was typically applied for UAV relays and achieved acceptable outage performance. Meanwhile, the outage probability and throughput closed-form expressions were derived. The derivations and analysis results showed that the proposed multiple parameters joint consideration can effectively improve the system throughput and reduce the system outage probability.

APENDIX

By invoking (15) into (19), it can be expressed the outage probability as

$$OP_{U_1}^{DF} = \Pr\left(|h_{SR}|^2 < \frac{\gamma_{th1}\left(|h_{RU_1}|^2+1\right)}{(a_1-\gamma_{th1}a_2)\rho|h_{RU_1}|^2}\right) \tag{25}$$

Based on probability density function (PDF) of $|h_i|^2$ is given as $f_{|h_i|^2}(x) = \lambda_{RU_1}e^{-\lambda_{RU_1}x}$, it can be rewritten as

$$\begin{aligned} OP_{U_1}^{DF} &= \int_0^\infty f_{|h_{RU_1}|^2}(x) \int_{\frac{\gamma_{th1}(x+1)}{(a_1-\gamma_{th1}a_2)\rho x}}^\infty f_{|h_{RU_1}|^2}(y)dxdy \\ &= \int_0^\infty \left(1 - e^{-\frac{\gamma_{th1}(x+1)}{(a_1-\gamma_{th1}a_2)\rho x}}\right)\lambda_{RU_1}e^{-\lambda_{RU_1}x}dx \end{aligned} \tag{26}$$

Thus, based on [25, 3.324.1] $OP_{U_1}^{DF}$ can be obtained as

$$\begin{aligned} OP_{U_1}^{DF} &= \int_0^\infty \left(1 - e^{-\frac{\gamma_{th1}(x+1)}{(a_1-\gamma_{th1}a_2)\rho x}}\right)\lambda_{RU_1}e^{-\lambda_{RU_1}x}dx \\ &= 1 - 2e^{-\frac{\lambda_{SR}\gamma_{th1}}{(a_1-\gamma_{th1}a_2)\rho}}\sqrt{\frac{\gamma_{th1}\lambda_{SR}\lambda_{RU_1}}{(a_1-\gamma_{th1}a_2)\rho}}K_1\left(2\sqrt{\frac{\gamma_{th1}\lambda_{RU_1}\lambda_{SR}}{(a_1-\gamma_{th1}a_2)\rho}}\right) \end{aligned} \tag{27}$$

It is end of the proof.

ACKNOWLEDGEMENT

The acknowledgment section is optional. The funding source of the research can be put here.

REFERENCES

[1] Y. Zeng, R. Zhang, and T. J. Lim, "Wireless communications with unmanned aerial vehicles: Opportunities and challenges," *IEEE Commun. Mag.*, vol. 54, no. 5, pp. 36-42, May 2016.

[2] A. Osseiran et al., "Scenarios for 5G mobile and wireless communications: The vision of the METIS project," *IEEE Commun. Mag.*, vol. 52, no. 5, pp. 26-35, May 2014.

[3] B. Ji, Y. Wang, B. Xing, Y. Wang, K. Song, C. Li, and R. Zhao, "Efficient protocol design for device-to-device communication in ultra dense networks," *Presented at the Int. Symp. Intell. Signal Process. Commun. Syst. (ISPACS)*, 2017.

[4] L. Gupta, R. Jain, and G. Vaszkun, "Survey of important issues in UAV communication networks," *IEEE Commun. Surveys Tuts., vol. 18, no. 2, pp. 1123-1152, 2nd Quart.*, 2015.

[5] M. Hua, Y. Wang, Z. Zhang, C. Li, Y. Huang, and L. Yang, "Power-efficient communication in UAV-aided wireless sensor networks," *IEEE Commun. Lett.*, vol. 22, no. 6, pp. 1264-1267, Jun. 2018.

[6] Y. Zeng and R. Zhang, "Energy-efficient UAV communication with trajectory optimization," *IEEE Trans. Wireless Commun.*, vol. 16, no. 6, pp. 3747-3760, Jun. 2017.

[7] C. Li, P. Liu, C. Zou, F. Sun, J. M. Cioffi, and L. Yang, "Spectral-efficient cellular communications with coexistent one- and two-hop transmissions," *IEEE Trans. Veh. Technol.*, vol. 65, no. 8, pp. 6765-6772, Aug. 2016.

[8] Dinh-Thuan Do and M.-S. Van Nguyen, "Device-to-device transmission modes in NOMA network with and without Wireless Power Transfer," *Computer Communications*, vol. 139, pp. 67-77, May 2019.

[9] D.-T. Do and A.-T. Le, "NOMA based cognitive relaying: Transceiver hardware impairments, relay selection policies and outage performance comparison," *Computer Communications*, vol. 146, pp. 144-154, 2019.

[10] D.-T. Do, A.-T. Le and B.-M. Lee, "On Performance Analysis of Underlay Cognitive Radio-Aware Hybrid OMA/NOMA Networks with Imperfect CSI," *Electronics*, vol. 8, no. 7, 2019.

[11] Dinh-Thuan Do and C.-B. Le, "Application of NOMA in Wireless System with Wireless Power Transfer Scheme: Outage and Ergodic Capacity Performance Analysis," *Sensors*, vol. 18, no. 10, 2018.

[12] T.-L. Nguyen and Dinh-Thuan Do, "Exploiting Impacts of Intercell Interference on SWIPT-assisted Non-orthogonal Multiple Access," *Wireless Communications and Mobile Computing*, vol. 2018, 2018.

[13] D-T. Do et al. ”Wireless power transfer enabled NOMA relay systems: two SIC modes and performance evaluation,” *TELKOMNIKA Telecommunication, Computing, Electronics and Control,* vol. 17, no. 6, pp. 2697-2703, 2019.

[14] Dinh-Thuan Do, Chi-Bao Le, A.-T. Le, ”Cooperative underlay cognitive radio assisted NOMA: secondary network improvement and outage performance,” *TELKOMNIKA Telecommunication, Computing, Electronics and Control,* vol. 17, no. 5, pp. 2147-2154, 2019.

[15] D.-T. Do, M. Vaezi and T.-L. Nguyen, ”Wireless Powered Cooperative Relaying using NOMA with Imperfect CSI,” *Proc. of IEEE Globecom Workshops (GC Wkshps),* pp. 1-6, 2018.

[16] D.-T. Do, A.-T. Le, C.-B. Le and B. M. Lee, ”On Exact Outage and Throughput Performance of Cognitive Radio based Non-Orthogonal Multiple Access Networks With and Without D2D Link,” *Sensors (Basel),* vol. 19, no. 15, 2019.

[17] X. Li, J. Li, Y. Liu, Z. Ding and A. Nallanathan, ”Residual Transceiver Hardware Impairments on Cooperative NOMA Networks,” *IEEE Transactions on Wireless Communications*, vol. 19, no. 1, pp. 680-695, Jan. 2020.

[18] X. Li, J. Li and L. Li, ”Performance Analysis of Impaired SWIPT NOMA Relaying Networks Over Imperfect Weibull Channels,” *IEEE Systems Journal,* vol. 14, no. 1, pp. 669-672, March 2020.

[19] X. Li, M. Liu, C. Deng, P. T. Mathiopoulos, Z. Ding and Y. Liu, ”Full-Duplex Cooperative NOMA Relaying Systems With I/Q Imbalance and Imperfect SIC,” *IEEE Wireless Communications Letters*, vol. 9, no. 1, pp. 17-20, Jan. 2020.

[20] X. Li, Qunshu Wang, Hongxing Peng, Hui Zhang, Dinh-Thuan Do, Khaled M. Rabie, Rupak Kharel and Charles C. Cavalcante, “A Unified Framework for HS-UAV NOMA Network: Performance Analysis and Location Optimization,” *IEEE Access,* vol. 8, pp. 13329-13340, 2020.

[21] X. Li, J. Li, L. Li, J. Jin, J. Zhang and D. Zhang, ”Effective Rate of MISO Systems Over $\kappa - \mu$ Shadowed Fading Channels,” *IEEE Access,* vol. 5, pp. 10605-10611, 2017.

[22] X. Li, M. Liu, C. Deng, , D. Zhang, X. Gao, K. M. Rabie, R. Kharel, “Joint Effects of Residual Hardware Impairments and Channel Estimation Errors on SWIPT Assisted Cooperative NOMA Networks,” *IEEE Access,* pp.1-15, 2019.

[23] X. Li, M. Huang, C. Zhang, D. Deng, K. M Rabie, Y. Ding, and J. Du, ”Security and Reliability Performance Analysis of Cooperative Multi-Relay Systems With Nonlinear Energy Harvesters and Hardware Impairments,” *IEEE Access,* vol. 7, pp. 102644-102661, 2019.

[24] J. Li, X. Li, Y. Liu, C. Zhang, L. Li and A. Nallanathan, ”Joint Impact of Hardware Impairments and Imperfect Channel State Information on Multi-Relay Networks,” *IEEE Access,* vol. 7, pp. 72358-72375, 2019.

[25] I. S. Gradshteyn and I. M. Ryzhik, ”Table of Integrals, Series and Products,” *6th ed. New York, NY, USA: Academic Press,* 2000.